Chapter 3

Process Design

This chapter describes the implementation of a Spray ILGAR process which is capable of depositing $CuInS_2$ thin films at a rate of about 20-30 nm per minute. Firstly, the development of a process is described which is suitable for the deposition of copper sulfide ($Cu_{2-x}S$, $0 \leq x \leq 0.2$) thin films (section 3.1.). In the next section, this setup is used for the deposition of indium-containing $In_2(O,S)_3$ thin films (section 3.2.). In section 3.3., two different approaches for the deposition of $CuInS_2$ thin films are evaluated: Firstly, the sequential deposition of $Cu_{2-x}S$ and $In_2(O,S)_3$ thin films is discussed (section 3.3.1.). Afterwards, the deposition of $CuInS_2$ thin films from a mixed solution of suitable copper and indium precursor compounds is investigated (section 3.3.2.).
The Spray ILGAR $CuInS_2$ thin films which are the subject of this thesis are meant to be used as absorber films in planar thin-film solar cells (section 6.1.). Since crystalline defects, such as dislocations, grain boundaries etc. may act as recombination sites in solar cells [Schock '01; Gloeckler '05] and can lead to a lowering of the photovoltaic performance, a high degree of crystalline order is needed. Therefore, the Spray ILGAR setup (Fig. 2.8), as developed by Allsop *et al.* [Allsop_1 '06] served as a starting point for the work presented in this thesis. The homogeneity of the thin films deposited by these authors was regarded to be a prerequisite for the deposition of planar $CuInS_2$ thin-film solar cell absorbers.
As mentioned in section 2.3., the deposition rate of the Spray ILGAR process as developed by Allsop *et al.* was too low for the deposition of 2 µm thick absorber films, as are needed for planar thin-film solar cells (section 6.1.). Therefore, the process had to be modified in order to increase the deposition rate to about 20-30 nm per minute (2 µm in 1-2 hours), which was regarded to be sufficient for a novel deposition process. Furthermore, the deposition of copper compounds could not be realized at all with the setup shown in Fig. 2.8. Hence, it was necessary to develop a process which is capable of depositing not only indium, but also copper compounds. Then, according to the Cu-In-S phase diagram (Fig. 2.4), also the formation of $CuInS_2$ is possible.

A list of the detailed preparation parameters of all samples which are mentioned in the following can be found in Appendix I. For all samples, 25 x 25 mm² soda-lime glass substrates with a sputtered molybdenum cover film of about 1 µm thickness were used. A 95 % Ar/5 % H_2S gas mixture was used as reactant gas in the Spray ILGAR process instead of 100 % H_2S, in order to avoid the risk of explosions due to the elevated substrate temperatures.
The deposited thin films are characterized by X-ray diffraction (XRD), scanning electron microscopy (SEM), X-ray fluorescence analysis (XRF) and elastic recoil detection analysis (ERDA), in order to identify the deposited phases (XRD) and to investigate the morphology (SEM) and composition (XRF, ERDA) of the films. These analysis techniques are explained in Appendix VII.

3.1. Deposition of Spray ILGAR Copper Sulfide Thin Films

In this section, the implementation of a Spray ILGAR process for the deposition of copper sulfide thin films as a prerequisite for the deposition of $CuInS_2$ thin films is described. By the choice of an appropriate copper precursor compound (copper hexafluoroacetylacetonate hydrate; section 3.1.1.) and solvent (acetone; section 3.1.2.) the deposition of copper sulfide thin films could be realized. The deposition rate was further increased by preheating the aerosol (section 3.1.3.). In combination, these modifications allowed the deposition of copper sulfide thin films at a rate of up to 11 nm per minute. At the end of the section these films are characterized by XRF, ERDA, SEM and ERDA (section 3.1.4.).
In order to enable the deposition of copper sulfide thin films, it was necessary to find a solution of appropriate copper compounds and solvents. The spraying solution needs to fulfill three prerequisites: Firstly, the copper compound has to be *soluble in the solvent*; secondly, the *nebulization of the solution* must be possible. Finally, a *copper-containing species needs to be deposited* in the spray step of the ILGAR-cycle from the aerosol droplets onto the substrate. Especially the latter is a challenging requirement, since initially no copper-containing compounds could be deposited using the setup shown in Fig. 2.8 [Allsop_2 '05].

3.1.1. Choice of a Copper-Containing Precursor Compound

The first step in the development of a Spray ILGAR process for the deposition of copper sulfide thin films was the choice of an appropriate copper-containing precursor compound for the spraying solutions. In the following, the arguments that led to the choice of copper (II) hexafluoroacetylacetonate hydrate are discussed. Afterwards, the applicability of such spraying solutions for the deposition of copper sulfide thin films is tested by preparing first copper sulfide thin films. By varying the substrate temperature and the spray step duration, the deposition of Spray ILGAR copper sulfide thin films could be realized.
As described in section 2.3., the growth mechanism of the Spray ILGAR process (deposition of a solid precursor compound and sulfurization of the same in separate process steps) is similar to that of ALD (section 2.2). Hence, precursor compounds which are used in ALD processes may also be an appropriate choice for the Spray ILGAR process. In ALD processes for the deposition of copper-containing compounds, such as copper sulfides or oxides, metal-organic compounds of copper are commonly used as precursors [Reijnen '03; Nanu '04; Törndahl '04]. These compounds consist of metal atoms which are weakly bound to organic groups so that the copper atoms can easily be deposited. A common metal organic copper precursor which is used for copper thin film deposition is copper (II) hexafluoroacetyl-acetonate or its hydrate (abbreviated as $Cu(hfac)_2$ in the following) [Reijnen '03; Törndahl '04]. The molecular formula of this compound is $Cu(CF_3COCHCOCF_3)_2 \cdot (H_2O)_x$ with $x < 1$. Its structure is shown in Fig. 3.1. Subsequently, the applicability of this compound for the deposition of copper sulfide thin films using the Spray ILGAR method is discussed.

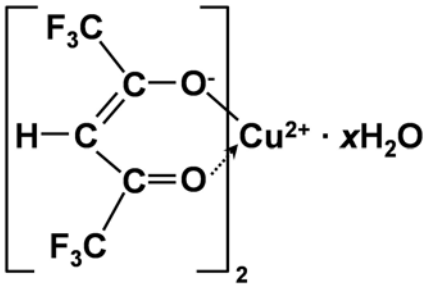

Fig. 3.1: Structure of the metalorganic copper compound copper (II) hexafluoroacetylacetonate hydrate ($Cu(hfac)_2$)

The Spray ILGAR process for In_2S_3 thin film deposition (section 2.3; Table 2.4) as developed by Allsop *et al.* [Allsop_1 '06] served as a starting point for the development of a Spray

ILGAR process for the deposition of copper sulfide thin films using $Cu(hfac)_2$. Therefore, the setup shown in Fig. 2.8 was used and the parameters stated in Table 3.1 were taken from the In_2S_3 deposition process without any variation. In particular, ethanol was initially used as a solvent in analogy to the In_2S_3-process. The molarity of the solution was empirically chosen as 10 mM instead of 25 mM, since $Cu(hfac)_2$ did not dissolve as well in ethanol as $InCl_3$. At this molarity, also the nebulization of the solution was possible. The substrate temperature and the duration of the spray step in the ILGAR-cycle were varied in order to find process conditions that enabled the deposition of Spray ILGAR copper sulfide thin films.

Table 3.1: Process parameters of the Spray ILGAR process for the deposition of copper sulfide thin films that were taken from the Spray ILGAR process for the deposition of In_2S_3 thin films (section 2.3; Table 2.4 without any variations.

Solvent	N_2 flow rate [l/min]	H_2S flow rate [l/min]	Duration of H_2S step [sec]	Pause after spray step [sec]	Pause after H_2S step [sec]
Ethanol	5.5	1.3	20	10	10

A first sample series (sample 301-305; Table 3.2) was prepared in order to investigate the influence of the substrate temperature (250 °C, 350 °C, 400 °C, 430 °C) and of the spray step duration (10 s and 30 s) on the deposition rate. In order to compare the thickness of these samples, a constant amount of solution was sprayed until it was completely used up. These samples were investigated by XRF using the Cu_2S-calibration described in Appendix VII.iii. Samples 302 and 305 were also investigated by ERDA in order to check the reliability of the XRF results.

Table 3.2: Influence of the preparation parameters on the composition and deposition rate of Spray ILGAR copper sulfide thin films prepared from $Cu(hfac)_2$/ethanol solutions: Substrate temperature, duration of the ILGAR spray step, number of cycles, nominal Cu_2S thickness and [Cu]:[S] ratio of the deposited thin films as determined by XRF and ERDA (Appendix VII.iii and VII.v) and the calculated deposition rate for samples 301-305. A 10 mM $Cu(hfac)_2$/ethanol solution was used for the preparation of these samples. The setup shown in Fig. 2.8 was used for deposition. For the preparation of each sample, 25 ml of spraying solution were completely consumed. The complete deposition parameters are listed in Appendix I. The uncertainty of the thickness is about 15 % (Appendix VII.iii).

Sample	Substrate temperature [°C]	Spray step [sec]	Number of ILGAR-cycles	Nominal Cu_2S thickness [nm]		[Cu]:[S] ratio		Deposition rate [nm/min]
				(XRF)	*(ERDA)*	*(XRF)*	*(ERDA)*	
Sample 301	250	10	30	1	/	1.4	/	< 0.1
Sample 302	350	10	31	11	10	1.6	1.1	0.4
Sample 303	400	10	35	12	/	1.7	/	0.4
Sample 304	400	30	18	17	/	0.9	/	0.8
Sample 305	430	30	22	19	25	1.0	1.7	0.7

It can be seen from Table 3.2 that the nominal Cu_2S thickness values determined by XRF and ERDA agree well within a relative error of 15 %. In contrast, the [Cu]:[S] ratios deviate by up to 70 %. This might be due to several reasons: Firstly, the investigated samples were very thin compared to the information depth of XRF and ERDA (1-2 µm). Therefore, the partial overlap of the S K_α X-rays and Mo L_α X-rays may increase the uncertainty of the XRF-determined sulfur content. Secondly, by ERDA it was found that the thin films are contaminated by carbon, oxygen and hydrogen (sample 302: 5 ± 1 % carbon, 6 ± 1 % oxygen, 5 ± 1 % hydrogen; sample 305: 5 ± 1 % carbon, 5 ± 1 % oxygen, 7 ± 1 % hydrogen). The presence of these contaminants might also influence the XRF determination of the sulfur content by absorption of the S K_α X-rays. However, at this stage of development of the Spray ILGAR process for copper sulfide thin film deposition, the [Cu]:[S] ratio of the deposited

layers is only of minor importance, since the focus lies on increasing the deposited amount of copper. Therefore, in Fig. 3.2 the influence of the substrate temperature on the nominal Cu_2S thickness (Fig. 3.2a) as well as on the Cu K_α count rate (Fig. 3.2b) is shown[3]. The positive influence of a high substrate temperature is most likely due to the fact that it accelerates the decomposition of the precursor, i.e. the breaking of the Cu-hfac bond ($T_{decomposition}$ ($Cu(hfac)_2$) = 300 °C [Naik '95]), in the vicinity of the substrate. Consequently, more material can be deposited. Furthermore, it was found empirically that an increase of the spray step duration in the ILGAR-cycle also increased the thickness of the deposited layer.

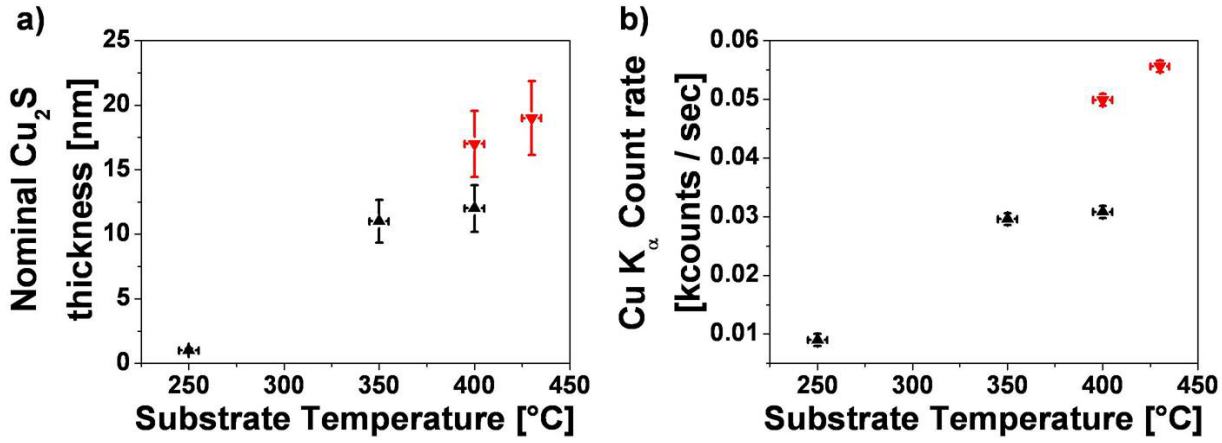

Fig. 3.2: Temperature dependence of the thickness of Spray ILGAR copper sulfide thin films deposited from $Cu(hfac)_2$/ethanol solutions: a) Nominal Cu_2S thickness of samples 301-305 (Table 3.2), which were deposited at different substrate temperatures. Samples 301-303 (▲) were deposited using a spray step of 10 s in the ILGAR-cycle, whereas samples 304 and 305 were deposited using a spray step of 30 s (▼). The thickness was measured by XRF using a Cu_2S calibration (Appendix VII.iii); b) Cu K_α count rates of the same samples as measured by XRF

In conclusion, these results show that the use of $Cu(hfac)_2$/ethanol spraying solutions allow the deposition of Spray ILGAR copper sulfide thin films. However, the deposition rates for samples 301-305 are all below 1 nm per minute and thus much lower than the desired rate of about 20-30 nm per minute. Thus, further modifications of the process are necessary in order to increase the deposition rate. Since the setup shown in Fig. 2.8 could only be used at substrate temperatures of up to 430 °C (due to the welding of the substrate heater), the deposition rate could not be increased by a further increase of the substrate temperature. Another possibility to increase the deposition rate may lie in the choice of a solvent that allows for a stronger nebulization of the solution and thus for an increased mass transfer from the solution to the substrate. This is the focus of the next section.

3.1.2. Choice of Solvent

In this section, the dependence of the deposition rate of the Spray ILGAR process for copper sulfide thin films on the choice of solvents is investigated. It is shown that the deposition rate is determined by the saturated vapor pressure, the surface tension and the dynamic viscosity of the solvent.
In the Spray ILGAR process, the material transport from the spraying solution to the substrate occurs via the formation of an aerosol by an ultrasonic source (section 2.3.). The deposition rate at the substrate depends on the amount of material that is transported to the substrate. Hence, a maximum nebulization rate is beneficial if a maximum deposition rate is desired.

[3] Both quantities are shown, since the [Cu]:[In] ratios determined by XRF (Table 3.2) deviate from that of Cu_2S, whose density is used for the thickness calculations in the XRF calibration routine (Appendix VII.iii).

The quantity of aerosol produced by ultrasonic nebulization at a constant power level of the ultrasonic source is a monotonically increasing function of the following ratio r [Langlet '93]:

$$r = \frac{p_s}{\sigma_{surf} \cdot \eta_{vis}} \qquad \text{Eq. (3.1)}$$

Here p_s is the saturated vapor pressure of the liquid (in mmHg), σ_{surf} is its surface tension (in mN/m), and η_{vis} is the dynamic viscosity (in cp). In Table 3.3, these values are listed for water, isopropanol, ethanol, acetonitrile, tetrahydrofuran and acetone, which were used as solvents for the Spray ILGAR process. These solvents were chosen, since they cover a wide range of r-values of almost two orders of magnitude (Table 3.3).

Table 3.3: Saturated vapor pressure, surface tension, dynamic viscosity and ratio r (Eq. 3.1) of water, isopropanol, ethanol, acetonitrile, tetrahydrofuran and acetone, which were used for the preparation of Spray ILGAR copper sulfide thin films.

Solvent	**Saturated vapor pressure p_s [mmHg]**	**Surface tension σ_{surf} [mN/m]**	**Dynamic viscosity η_{vis} [cp]**	**Ratio r**	**References**
Water	24	72	1.00	0.3	[Langlet '93]
Isopropanol	33	22	2.26	0.7	[Sigma_1 '08], [www_1 '08], [Weast '70]
Ethanol	44	23	1.19	1.6	[Langlet '93]
Acetonitrile	73	29	0.39	6.4	[Sigma_1 '08], [www_1 '08], [www_5 '05]
Tetrahydrofuran	143	26	0.47	11.5	[Sigma_1 '08], [www_1 '08], [www_5 '05]
Acetone	185	24	0.32	24.3	[Langlet '93]

The ratio r, which determines the nebulization rate, exhibits a maximum value of 24.3 for acetone and a minimum value of 0.3 for water. For ethanol, which has been used so far for the Spray ILGAR process, the ratio r equals 1.6. Therefore, it can be assumed that the nebulization rate and also the deposition rate increases, if acetone is used instead of ethanol. However, the values in Table 3.3 are only valid for the pure solvents and may change upon the addition of $Cu(hfac)_2$. This was tested by preparing a series samples (samples 306-311) from 10 mM $Cu(hfac)_2$ solutions in water, isopropanol, ethanol, acetonitrile, tetrahydrofuran and acetone, respectively. Table 3.4 lists the results obtained from this series of samples.

Table 3.4: Effect of using various solvents (water, isopropanol, ethanol, acetonitrile, tetrahydrofuran and acetone) on the properties of Spray ILGAR copper sulfide films (samples 306-311): Number of ILGAR-cycles, nominal Cu_2S thickness, [Cu]:[S] ratio and deposition rate as measured by XRF (Appendix VII.iii). The films were each prepared from 25 ml of a 10 mM $Cu(hfac)_2$ solution. The substrate temperature was 430 °C. The durations of the spray- and H_2S step were 30 s and 20 sec, respectively. The complete preparation parameters are listed in Appendix I. The relative uncertainties of the film thickness and deposition rate are 15 %.

Sample	**Solvent**	**Number of ILGAR-cycles**	**Nominal Cu_2S Thickness [nm]**	**[Cu]:[S] ratio**	**Deposition rate [nm/min]**
Sample 306	Water	*No nebulization*			
Sample 307	Isopropanol	*No nebulization*			
Sample 308	Ethanol	22	19	1.0	0.7
Sample 309	Acetonitrile	16	49	1.4	2.6
Sample 310	Tetrahydrofuran	14	49	1.4	3.0
Sample 311	Acetone	9	48	1.4	4.6

These results agree well with the behavior expected from the values in Table 3.3. No nebulization at all was observed for the aqueous (sample 306) and isopropanol (sample 306) solutions. These solvents exhibit the smallest r-values of 0.33 and 0.67 in Table 3.3, respectively. For the sample deposited from an ethanol solution (sample 308) the nebulization

was possible, though it was much stronger for the acetonitrile (sample 309), tetrahydrofuran (sample 310), and acetone (sample 311) solutions. The deposition rate also exhibited the same trend as ratio *r* in Table 3.3. Thus, a maximum deposition rate of 4.6 ± 0.7 nm per minute was achieved for deposition from a $Cu(hfac)_2$/acetone solution. This corresponds to an increase of the deposition rate of a factor of about seven compared to the use of ethanol solutions. It can also be seen from Table 3.4 that the thin films deposited from acetonitrile (sample 309), tetrahdrofuran (sample 310) and acetone solutions (sample 311) all exhibit a similar thickness of about 49 ± 7 nm and a [Cu]:[S] ratio of 1.4 ± 0.1. The latter indicates that copper-rich phases like Cu_2S or Cu_9S_5 (section 2.1.3.) are present in the films. Since a maximum deposition rate is desired for the Spray ILGAR process for the deposition of copper sulfide, only $Cu(hfac)_2$/acetone solutions were used in the following. However, the deposition rate of about 5 nm per minute obtained for sample 311 is still below the desired rate of 20-30 nm per minute. Therefore, in the next section modifications of the Spray ILGAR setup are described, which led to a further increase of the deposition rate.

3.1.3. Modifications of the Spray ILGAR Setup

In this section, the Spray ILGAR setup developed by Allsop *et al.* [Allsop_1 '06] (Fig. 2.8) is modified in order to further increase the deposition rate of the Spray ILGAR process for the deposition of copper sulfide thin films. In particular, the influence of preheating the aerosol and of the nitrogen carrier gas flow rate on the deposition rate is discussed.
It was shown (section 3.1.1.) that a high substrate temperature increases the deposition rate, since it enhances the decomposition of the precursor in the vicinity of the substrate and thus enables the deposition of more material. However, in the setup shown in Fig. 2.8, the aerosol is not heated before it reaches the substrate. Thus, the aerosol droplets are still in the same state as directly after their generation. The mean droplet size *d* (in cm) of an aerosol, which was nebulized by an ultrasonic source is given in Ref. [Langlet '93; Kodas '99]:

$$d = \left(\frac{\pi \cdot \sigma_{\text{surf}}}{4 \cdot \rho \cdot f_{\text{us}}^{\,2}} \right)^{1/3} \qquad \text{Eq. (3.2)}$$

Here, σ_{surf} is the surface tension (in mN/m), ρ is the fluid density (in g/cm^3), and f_{us} is the frequency of the ultrasonic source (in Hz). For a frequency of f_{us} = 1.65 MHz as it is used in this thesis, Eq. (3.2) yields a mean droplet size of 2.05 µm for acetone. In Table 3.5, the mean droplet sizes are also given for water, isopropanol, ethanol, acetonitrile and tetrahydrofuran. Similar values between 2.00 µm and 2.75 µm are obtained for all these solvents.

Table 3.5: Surface tensions, densities and calculated mean droplet sizes (Eq. (3.2)) of aerosols formed from water, isopropanol, ethanol, acetonitrile, tetrahydrofuran and acetone by ultrasonic nebulization at a frequency of f_{us} = 1.65 MHz.

Solvent	Surface tension σ_{surf} [mN/m]	Density ρ [g/cm^3]	Droplet size *d* [µm]	References
Water	72	1.000	2.75	[Langlet '93]
Isopropanol	22	0.786	2.00	[Sigma_1 '08], [www_1 '08]
Ethanol	23	0.789	2.03	[Langlet '93]
Acetonitrile	29	0.786	2.21	[Sigma_1 '08], [www_1 '08]
Tetrahydrofuran	26	0.889	2.05	[Sigma_1 '08], [www_1 '08]
Acetone	24	0.790	2.05	[Langlet '93]

Generally, the surface-to-mass ratio increases for aerosol droplets of decreasing diameter. Hence, a smaller droplet size facilitates the evaporation of the solvent from the droplet and thereby also the subsequent thermal decomposition of the precursor compound $Cu(hfac)_2$.

Consequently, a smaller droplet size is advantageous for increasing the deposition rate of the Spray ILGAR process. It can be assumed that an additional preheating of the aerosol leads to an enhanced evaporation of the solvent, which reduces the droplet size. Thus, smaller droplets – still containing the same amount of the $Cu(hfac)_2$ – should arrive at the substrate. Then the evaporation of the residual amount of solvent in the temperature gradient near the substrate surface should be accelerated and consequently the decomposition rate of the $Cu(hfac)_2$-molecules should be enhanced. Furthermore, a sublimation temperature of $T_{sublimation}$ = 60 °C is reported for $Cu(hfac)_2$ [Törndahl '04]. Hence, after the evaporation of the solvent from the aerosol droplets, the sublimation of $Cu(hfac)_2$ can be expected for preheating temperatures in the range of 60 °C. Thus, the decomposition of the $Cu(hfac)_2$-molecules will take place from the gas phase, which should increase the homogeneity of the deposited films (section 2.3.). Therefore, the setup in Fig. 2.8 was modified by implementing a homemade aluminum tube (26 cm x 2.5 cm x 2.5 cm), in which the precursor mist is preheated to a temperature $T_{aerosol}$. In order to increase the aerosol heating effect of the tube, its inner volume was reduced by placing a piece of aluminum (26 cm x 2 cm x 2 cm) inside. Aluminum was the chosen material for this tube for two reasons: Firstly, it has a high thermal conductivity compared to other materials[4] and is still relatively inert to H_2S (in contrast to e.g. copper) [www_3 '06]. Secondly, it is easy to work with and allowed for customizing the tube to the Spray ILGAR setup. The modified Spray ILGAR setup for the deposition of copper sulfide thin films is shown in Fig. 3.3.

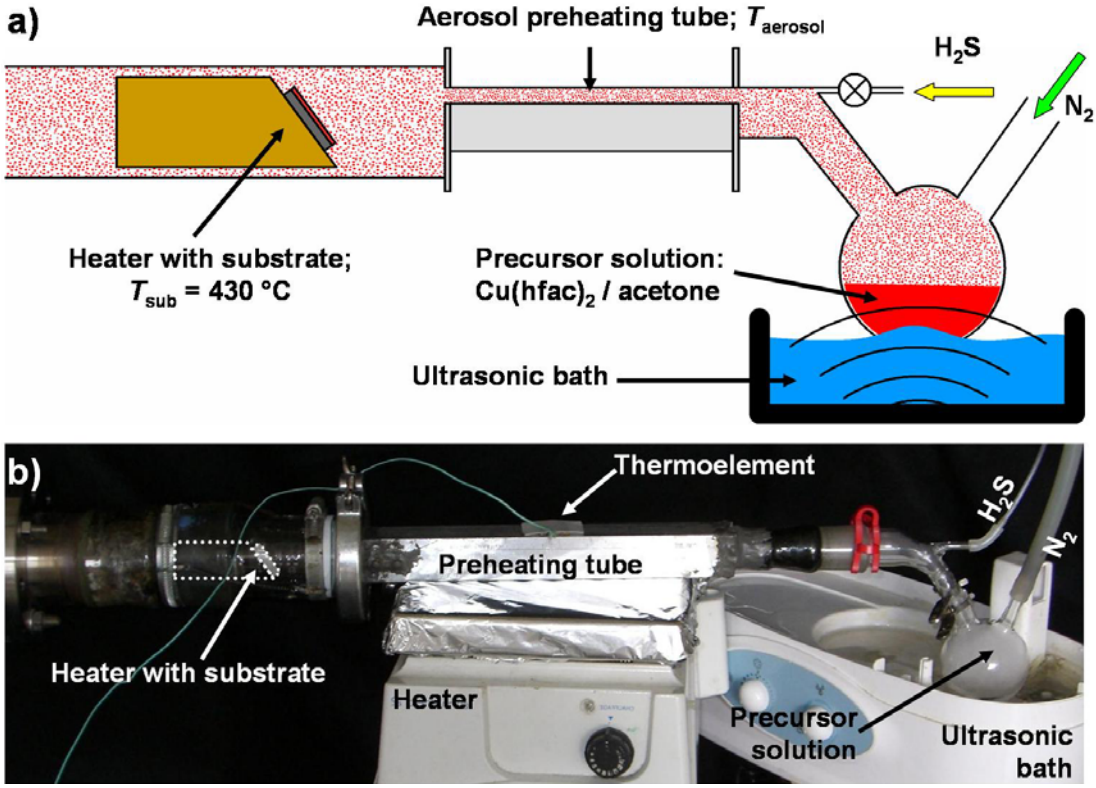

Fig. 3.3: a) Schematic sketch of the modified homemade Spray ILGAR setup for the deposition of copper sulfide thin films including a tube for the preheating of the aerosol; b) photograph of the same setup.

Obviously, the effect of the aerosol preheating depends on the preheating temperature $T_{aerosol}$ as well as on the flow rate of the nitrogen carrier gas stream, which determines the residence time of the aerosol droplets inside the preheating tube. Therefore, both parameters have been

[4] Thermal conductivities of aluminum, copper, iron and stainless steel at 20 °C: Aluminum: 204 $Wm^{-1}K^{-1}$; copper: 386 $Wm^{-1}K^{-1}$; iron: 73 $Wm^{-1}K^{-1}$; stainless steel: 12 $Wm^{-1}K^{-1}$ – 45 $Wm^{-1}K^{-1}$ [www_2 '05].

varied systematically in order to investigate their influence on the deposition rate. Two series of copper sulfide thin films were deposited onto molybdenum-coated glass substrates. In the first series, the nitrogen carrier gas flow rate was held constant at 3.3 l/min and the preheating temperature was varied between 70 °C and 200 °C (samples 312-317). In the second series, the preheating temperature was held constant at $T_{aerosol}$ = 100 °C, whereas the flow rate of the nitrogen carrier stream was varied between 1.1 l/min and 5.5 l/min (samples 318-322). Each of the samples of both series was prepared by spraying 25 ml of 10 mM $Cu(hfac)_2$/acetone solution until they were completely consumed. The durations of the spray- and H_2S steps of the ILGAR-cycle were set to 30 s and 20 s as in the previous experiments. The substrate temperature was 430 °C (Appendix I). Fig. 3.4a shows the nominal Cu_2S thickness of samples 312-317 as a function of the preheating temperature $T_{aerosol}$ (●). In Fig. 3.4b the nominal Cu_2S thickness of samples 318-322 is shown as a function of the nitrogen carrier gas stream flow rate (●). In order to quantify eventual losses of material due to the deposition of copper sulfide on the inner walls of the preheating tube, identical experiments were made, in which molybdenum-covered glass substrates were placed in the center of the preheating tube (samples 312i-322i). The nominal Cu_2S thickness of the films, which were deposited onto these substrates were measured by XRF and are also shown in Fig. 3.4a and b (▲).

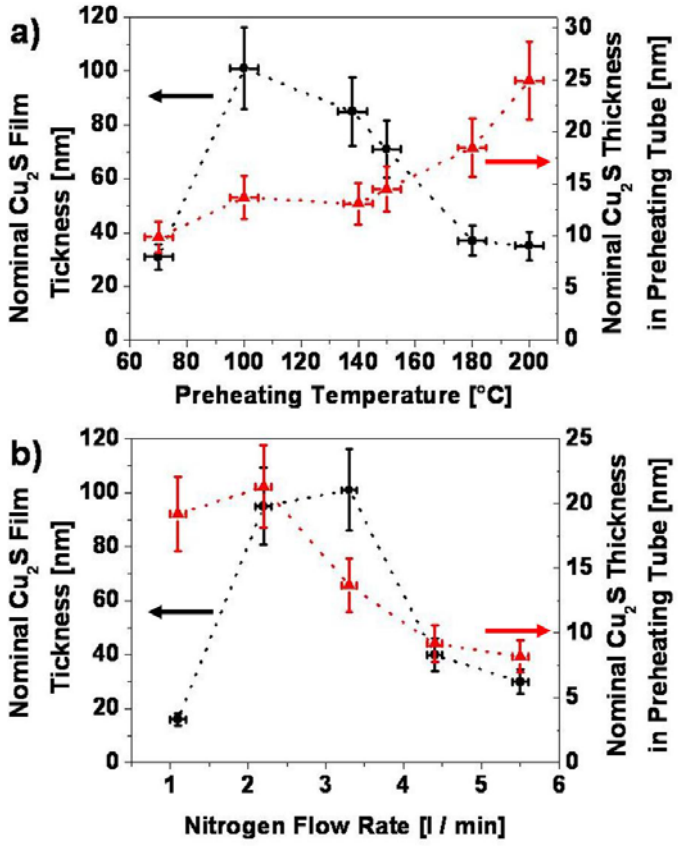

Fig. 3.4: Influence of the aerosol preheating on the deposition rate: Nominal Cu_2S thickness as measured by XRF (●) of Spray ILGAR copper sulfide thin films, which were deposited at a substrate temperature of 430 °C from 10 mM $Cu(hfac)_2$ / acetone solutions using the setup shown in Fig. 3.3. The durations of the spray- and H_2S steps in the ILGAR-cycle were 30 s and 20 sec, respectively. By XRF also the deposition inside the preheating tube was quantified (▲). For a) the nitrogen flow rate was set to 3.3 l/min and the preheating temperature was varied between 70 °C and 200 °C (samples 312-317 and 312i-317i). For b) the nitrogen flow rate was varied between 1.1 l/min and 5.5 l/min at a preheating temperature of 100°C (samples 318-322 and 318i-322i). See Appendix I for deposition parameters.

It can be seen from Fig. 3.4a and b that within these two series of copper sulfide thin films, a maximum thin film thickness of about 100 ± 15 nm is achieved for a nitrogen flow rate of 3.3 l/min and a preheating temperature of $T_{aerosol}$ = 100 °C (samples 313 and 320). This corresponds to a deposition rate of 9 ± 1 nm per minute.

That a maximum copper sulfide deposition is achieved for these medium values, can be understood, if the deposition on the inner walls of the preheating tube (samples 312i-322i) is taken into account. On the one hand, high preheating temperatures as well as low nitrogen carrier gas flow rates both result in an enhanced heating of the aerosol inside the preheating tube. The copper sulfide depositions on samples 312i-317i (▲ in Fig. 3.4a) and 318i-322i (▲ in Fig. 3.4b) show that both conditions cause an increased deposition of copper sulfide on the

inner walls of the tube. This deposited material is lost for the thin film deposition on the substrate. On the other hand, high nitrogen flow rates or low preheating temperatures do both not fully exploit the potential of the preheating step, since the aerosol is not heated strong enough to reach the optimum temperature for deposition. This also becomes apparent from Fig. 3.4a and b, since both, the deposition on the substrate and inside the preheating tube decrease for preheating temperatures below 100 °C (Fig. 3.4a) or nitrogen flow rates higher than 3.3 l/min (Fig 3.4b). The observed increase of the deposition for preheating temperatures over 70 °C, coincides with the boiling point of acetone (57 °C; [Lautenschläger '02]) and the sublimation temperature of $Cu(hfac)_2$ (60 °C; [Törndahl '04]) and thus confirms that the preheating leads to the evaporation of acetone and / or the decomposition of $Cu(hfac)_2$.
Additionally, a further increase of the deposition rate in the Spray ILGAR process for copper sulfide thin films was achieved by increasing the concentration from 10 mM to 40 mM. Thus, a 140 ± 21 nm thick copper sulfide thin film (sample 323) was deposited from 25 ml $Cu(hfac)_2$ / acetone solution in 11 ILGAR-cycles, which corresponds to a deposition rate of about 11 ± 2 nm per minute. Event though this rate is still below the range of 20-30 nm per minute that was desired for the deposition of Spray ILGAR $CuInS_2$ thin films, it enables the deposition of copper sulfide films, which can serve as a basis for the deposition of Spray ILGAR $CuInS_2$ thin films. Therefore, no further approaches were made in order to increase the deposition rate. The parameters for the Spray ILGAR process for copper sulfide thin films, which have been deduced in sections 3.1.1.-3.1.3., are summarized in Table 3.6. and will be used as standard parameters for the Spray ILGAR process in the following.

Table 3.6: Preparation parameters for the Spray ILGAR process for the deposition of copper sulfide thin films using the setup shown in Fig. 3.3. With these parameters, a deposition rate of 11 nm/min could be realized (sample 323).

Precursor compound	$Cu(hfac)_2$
Solvent	Acetone
Molarity [mM]	40
N_2 flow rate [l/min]	3.3
H_2S flow rate[l/min]	1.31
Substrate temperature [°C]	430
Preheating temperature [°C]	100
Duration of spray step [sec]	30
Duration of H_2S step [sec]	20
Pause after spray step [sec]	10
Pause after H_2S step [sec]	10

3.1.4. Characterization of Spray ILGAR Copper Sulfide Thin Films

In this section, the Spray ILGAR thin film (sample 323) deposited using the parameters deduced in section 3.1.3. (Table 3.6) is characterized with respect to composition, structure and morphology, in order to identify the deposited copper sulfide phases and to evaluate the applicability of such films as precursor films for the sequential deposition of $CuInS_2$ thin films. Therefore, sample 323 was investigated by XRF, ERDA, XRD and SEM. These methods are explained in Appendix VII.ii-v.
By XRF a thickness of 140 ± 21 nm and a composition of 65 ± 1 at. % copper and 35 ± 1 at. % was measured, which indicates that the thin film consists of copper-rich phases like Cu_2S, $Cu_{1.96}S$, Cu_9S_5, $Cu_{1.81}S$ or $Cu_{1.75}S$ (section 2.1.3.). Since the XRF-calibration used, was only sensitive to copper and sulfur, the film was also characterized by ERDA in order to obtain information about possible contaminants. By ERDA a composition of 64 ± 1 at. % copper, 31 ± 1 at. % sulfur, 2 ± 1 at. % oxygen, 2 ± 1 at. % carbon, < 1 at. % hydrogen and < 1 at. % fluorine were detected. The thickness was determined as 100 ± 15 nm assuming the density to equal the bulk density of Cu_2S (5.60 g/cm^3 [www_4 '08]). The [Cu]:[S] ratio agrees

well with the XRF results in spite of the presence of carbon, oxygen, hydrogen and traces of fluorine as contaminants. These elements probably stem from the ligands of the $Cu(hfac)_2$ compound that was used in the spraying solutions (section 3.1.1.).
The crystal structure of sample 323 was investigated by grazing incidence XRD (0.5 °). The diffractogram is shown in Fig. 3.5. Besides molybdenum from the substrate (JCPDS 00-042-1120; from the substrate) α-Cu_2S (JCPDS 01-0172-0171), $Cu_{1.81}S$ (JCPDS 00-041-0959) and Cu_9S_5 (JCPDS 00-026-0476) were identified as crystalline phases. All these phases have a [Cu]:[S] ratio close to two and thus agree well with the composition determined by XRF and ERDA. In the following, these phases are summarized as $Cu_{2-x}S$ ($0 \leq x \leq 0.2$).

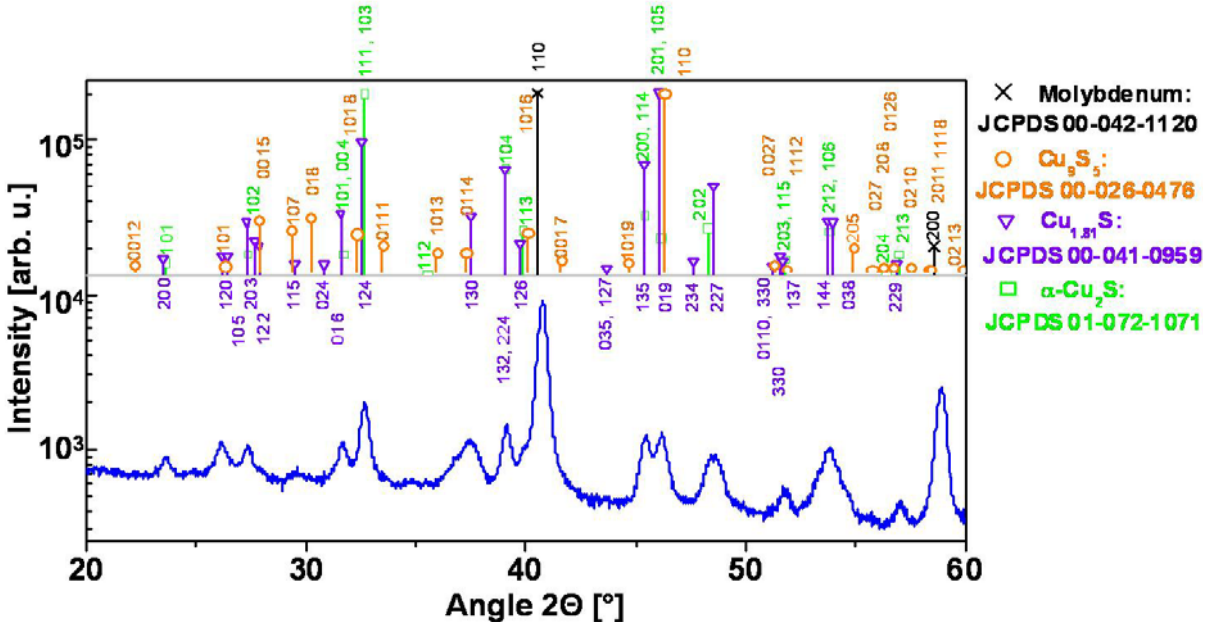

Fig. 3.5: Diffractogram (0.5 ° grazing incidence XRD) of a Spray ILGAR copper sulfide thin film (sample 323). This film was prepared from a 40 mMol $Cu(hfac)_2$/acetone solution using the deposition parameters listed in Table 3.6. The intensity is shown on a logarithmic scale. The reflections are assigned to the contributing phases according to JCPDS reference charts: Mo (JCPDS 00-042-1120), $Cu_{1.81}S$ (JCPDS 00-041-0959), α-Cu_2S (JCPDS 01-072-1071) and Cu_9S_5 (JCPDS 00-026-0476).

The morphology of sample 323 was investigated by means of SEM. The morphology is especially important, since the copper sulfide thin films are meant to be used for the preparation of planar $CuInS_2$ solar cell absorber films, for which a compact morphology is desired. In Fig. 3.6 a planar SEM image of sample 323 is shown.

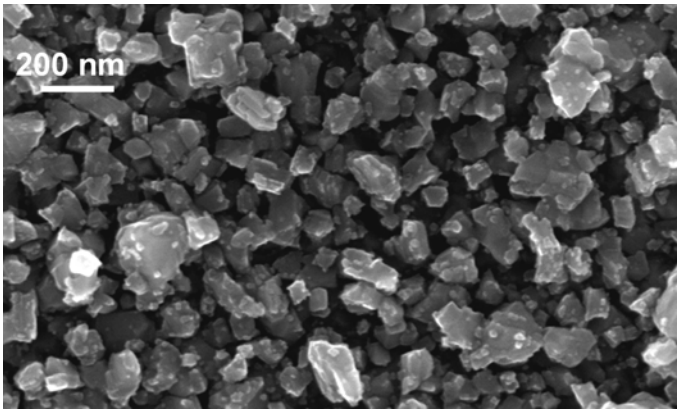

Fig. 3.6: Plan-view SEM image obtained from a Spray ILGAR copper sulfide thin film (sample 323) . This film was prepared from a 40 mMol $Cu(hfac)_2$/acetone solution using the deposition parameters listed in Table 3.6.

The film consists of crystallites with diameters of up to 200 nm. Even though voids are visible between these crystallites this Spray ILGAR copper sulfide layer is not highly structured but rather compact.

In view of the goal of preparing planar Spray ILGAR $CuInS_2$ solar cell absorbers, a compact morphology it is advantageous.

3.2. Deposition of Spray ILGAR Indium Oxide Sulfide Thin Films

In view of the goal to prepare $CuInS_2$ thin films from bilayers of $Cu_{2-x}S$ ($0 \leq x \leq 0.2$) and indium oxide sulfide ($In_2(O,S)_3$), the parameters, which have been deduced for the Spray ILGAR process for copper sulfide thin film deposition (Table 3.6), have been used for the deposition of $In_2(O,S)_3$ films in this section.
Sample 324 was prepared using the setup shown in Fig. 3.3 and the preparation parameters listed in Table 3.6, but instead of a 40 mM $Cu(hfac)_2$/acetone solution, a 40 mM $InCl_3$/ acetone solution was used. 25 ml of solution were sprayed until they were consumed completely (14 ILGAR-cycles).
The composition of the deposited thin film (sample 324) was investigated by ERDA. Thereby, it was found that the composition varied in depth (section 4.3.) with an integral composition of 37 ± 1 at. % indium, 34 ± 1 at. % oxygen, 25 ± 1 at. % sulfur, 2 ± 1 at. % hydrogen and 1 ± 1 at. % chlorine. This shows that the film does not consist of pure In_2S_3 as the Spray ILGAR thin films deposited by Allsop *et al.* [Allsop_1 '06]. However, the integral ratio of [In]:[O+S] = 0.62 ± 0.04 is close to the [cation]:[anion] ratio in In_2S_3 and In_2O_3 of 0.67, which indicates that the film consists of a blend of In_2S_3 and In_2O_3. This assumption was verified by grazing incidence XRD (0.5 °). The diffractogram obtained from this measurement is shown in Fig 3.7. The contributions of In_2S_3 (JCPDS 00-025-0390) and In_2O_3 (JCPDS 00-006-0416) can be distinguished. All peaks can either be assigned to the lattice planes of In_2S_3 or In_2O_3.

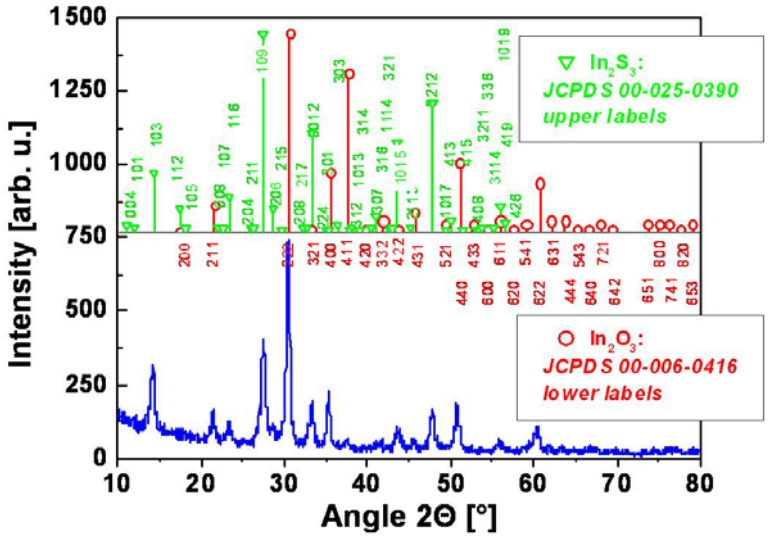

Fig. 3.7: X-ray Diffractogram (0.5 °) of a Spray ILGAR $In_2(O,S)_3$ thin film (sample 324); the reflections are assigned to the contributing phases according to JCPDS reference charts: In_2S_3 (JCPDS 00-025-0390); In_2O_3: (JCPDS 00-006-0416). The thin film was prepared from a 40 mM $InCl_3$/acetone solution (25 ml) using the setup shown in Fig. 3.3 and the parameters listed in Table 3.6.

The morphology of the same thin film (sample 324) was investigated by SEM in order to evaluate the applicability of such thin films for the sequential preparation of $CuInS_2$ thin-film solar cell absorbers. In Fig. 3.8, a SEM-image of the cross-section of sample 324 can be seen. The lower part of the film consists of a compact nanocrystalline layer of about 400-500 nm thickness, which is covered by a highly structured layer of similar thickness. The origin of this structure is not yet clear, but seems to be correlated to compositional changes (section 4.3.).
From the thickness of this film observed in Fig. 3.8 (sample 324), a deposition rate of about 30 nm per minute can be estimated for the deposition of Spray ILGAR $In_2(O,S)_3$ thin films. This value lies in the range of the rates of about 20-30 nm per minute, which are desired for the deposition of $CuInS_2$ thin films. However, the films contain about 34 % of oxygen and are highly structured, which may be problematic for the preparation of $CuInS_2$ thin films. In view of the application of bilayers of Spray ILGAR $In_2(O,S)_3$ and $Cu_{2-x}S$ thin films as precursor

layers for the preparation of $CuInS_2$ thin films, it would be beneficial to use pure and compact In_2S_3 thin films instead of the highly structured $In_2(O,S)_3$ thin films. Theoretically, this could be achieved by increasing the duration of the H_2S step in the ILGAR-cycle. It will be explained, however, that also this approach does not allow for the deposition of single phase In_2S_3 films with deposition rates in desired the desired range of 20-30 nm per minute (section 4.3.). Therefore, it was decided not to further modify the Spray ILGAR process for the deposition of $In_2(O,S)_3$ thin films but to rather focus on the implementation of a Spray ILGAR process for $CuInS_2$ thin film deposition (sections 3.3.1. and 3.3.2.).

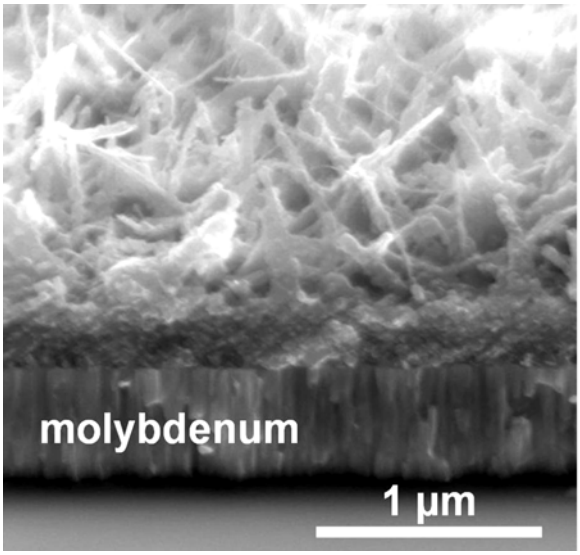

Fig. 3.8: Cross-sectional SEM image of a Spray ILGAR $In_2(O,S)_3$ thin film (sample 324). The image was obtained from a 45 °-tilted sample. The thin film was prepared from a 40 mM $InCl_3$/acetone solution (25 ml) using the setup shown in Fig 3.3 and the parameters listed in Table 3.6.

3.3. The Spray ILGAR Deposition Process for $CuInS_2$ Thin Films

In this section, two different approaches for the deposition of Spray ILGAR $CuInS_2$ thin films are evaluated. Since these films are meant to be used as absorber layers in planar thin-film solar cells, a compact morphology of the films as well as a deposition rate of 20-30 nm per minute is desired (section 2.3.). In section 3.3.1., a sequential process is used, in which Spray ILGAR $Cu_{2-x}S$ and $In_2(O,S)_3$ layers are sequentially deposited and subsequently annealed in an Ar/H_2S atmosphere. In the following section (section 3.3.2.), the direct deposition of $CuInS_2$ from a mixed solution of $Cu(hfac)_2$ and $InCl_3$ is discussed.

3.3.1. Sequential Deposition of Spray ILGAR $CuInS_2$ Thin Films

In this section, a sequential process for the preparation of $CuInS_2$ thin films from bilayer stacks of Spray ILGAR $Cu_{2-x}S$ and $In_2(O,S)_3$ layers is described. According to the Cu-In-S phase diagram (Fig. 2.4) $Cu_{2-x}S$ and In_2S_3 readily form $CuInS_2$ at a process temperature of 430 °C until one of the cation species is used up. Since the Spray ILGAR $In_2(S,O)_3$ thin films (section 3.2.) contain In_2O_3, the bilayer stacks were annealed in an Ar/H_2S atmosphere at 500 °C in order convert In_2O_3 to In_2S_3 and to enhance the formation of $CuInS_2$.
The sequential process investigated in this section is similar to a process developed by Bleyhl *et al.* [Bleyhl '99], who prepared $CuInS_2$ solar cell absorbers from sequentially PVD-deposited In_2S_3 and CuS layers. After deposition, these bilayers were annealed in a H_2S atmosphere between 400 °C and 600 °C, which led to the formation of $CuInS_2$.
In order to evaluate the applicability of a similar sequential process based on the Spray ILGAR method, three different stacking sequences of $Cu_{2-x}S$ and $In_2(O,S)_3$ layers were used, which are depicted schematically in Fig. 3.9.

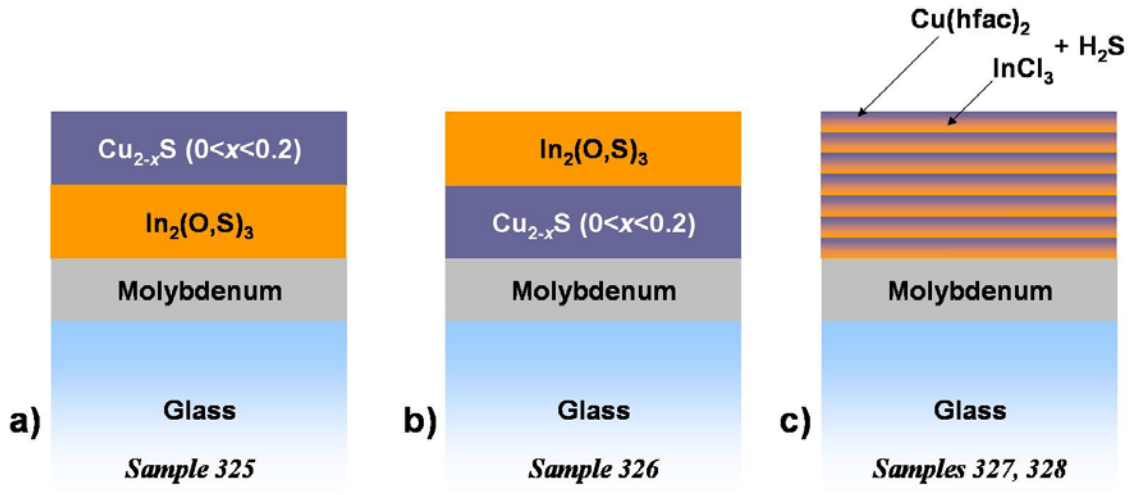

First 25 ml:
30 s $InCl_3$ / acetone spraying
10 s pause
20 s H_2S
10 s pause

Second 25 ml:
30 s $Cu(hfac)_2$ / acetone spraying
10 s pause
20 s H_2S
10 s pause

First 25 ml:
30 s $Cu(hfac)_2$ / acetone spraying
10 s pause
20 s H_2S
10 s pause

Second 25 ml:
30 s $InCl_3$ / acetone spraying
10 s pause
20 s H_2S
10 s pause

First and second 25 ml:
15 s $InCl_3$ / acetone spraying
10 s pause
15 s $Cu(hfac)_2$ / acetone spraying
20 s H_2S
10 s pause

Fig. 3.9: Different stacking sequences of Spray ILGAR $Cu_{2-x}S$ and $In_2(O,S)_3$ layers that were used for the preparation of $CuInS_2$ thin films and the corresponding ILGAR cycle sequences: a) a $Cu_{2-x}S$ layer (corresponding to 25 ml of solution) is deposited on top of an $In_2(O,S)_3$ layer (corresponding to 25 ml of solution) (sample 325); b) an $In_2(O,S)_3$ layer (corresponding to 25 ml of solution) is deposited on top of a $Cu_{2-x}S$ layer (corresponding to 25 ml of solution) (sample 326); c) $Cu(hfac)_2$/acetone and $InCl_3$/acetone are sprayed consecutively in the same ILGAR cycle prior to sulfurization. This cycle is repeated until 25 ml of each solution are consumed (samples 327 and 328). The detailed deposition parameters are listed in Appendix I.

In a first approach (Fig. 3.9a), a $Cu_{2-x}S$ layer was deposited on top of an $In_2(O,S)_3$ layer. Here, each layer was deposited by spraying 25 ml of the respective solution ($Cu(hfac)_2$ or $InCl_3$) using the parameters listed in Table 3.6 (sample 325). This is the same sequence as used by Bleyhl *et al.* [Bleyhl '99] and also coevaporation processes of highly efficient $CuInS_2$ solar cell absorbers start by evaporating an indium sulfide layer and subsequent coevaporation of copper and sulfur [Walter '96].
The inverted sequence, starting with the deposition of a $Cu_{2-x}S$ layer and subsequent deposition of an $In_2(O,S)_3$ layer (Fig. 3.9b), was also used. Again, 25 ml of the respective solution and the parameters listed in Table 3.6 were used for the deposition of each layer of the film (sample 326).
In a third approach (Fig. 3.9c), a sequence of several alternating bilayers was deposited. Here each bilayer was deposited in only one single ILGAR cycle, in which the $Cu(hfac)_2$/acetone and the $InCl_3$/acetone solution were sprayed after each other prior to sulfurization. Therefore, two vessels with the corresponding solutions were attached to the setup shown in Fig. 3.3. This last approach was tested in two modifications: Firstly, a molarity of 40 mM was used for both solutions (25 ml each). Hence, the nominal [Cu]:[In] ratio equaled one (sample 327) as in $CuInS_2$. Secondly, a reduced molarity of only 32 mM was chosen for the $InCl_3$/acetone solution in order to provide copper-rich conditions (sample 328), which have been found to favor the growth of well-crystallized $CuInS_2$ thin films in other deposition processes like PVD or RTP [Scheer '93; Klenk '97]. The deposition parameters in Table 3.6 were used.

After deposition all four samples (samples 325-328; Fig. 3.9a-c) were annealed in a 95 % Ar/ 5 % H_2S atmosphere in a standard quartz tube oven in order to sulfurize residual In_2O_3 and to enhance the formation of $CuInS_2$. The annealing profile (45 min at 375 °C in Ar and 15 min at 550 °C in Ar/H_2S) was the same as used by Kropp for the deposition of $CuInS_2$ thin films using the setup shown in Fig. 2.7 [Kropp '02]. After the annealing, the samples were etched in KCN in order to remove copper sulfide species, which might have segregated on the surface of the films. As mentioned in section 2.2., KCN etching is a common technique to remove such segregated phases in deposition processes of thin-film solar cells [Scheer '94; Scheer '95; Klaer '03; Klenk '05].
After KCN etching, the thin films (samples 325-328) were investigated by XRF in order to determine their composition. The calibration routine is described in Appendix VII.iii. and is only sensitive to copper, indium and sulfur. Hence, the measured contents are to be understood as relative contents of the respective elements. The corresponding values for samples 325-328 are listed in Table 3.7 together with the film thickness (assuming a bulk $CuInS_2$ thickness of 4.75 g/cm^3 [www_4 '08]) and the calculated deposition rates.

Table 3.7: Relative copper, indium and sulfur content (in atomic percent) and thickness (assuming a $CuInS_2$ bulk density of 4.75 g/cm^3 [www_4 '08]) of sequentially deposited Spray IGAR CuInS2 thin films (samples 325-328) after annealing in Ar/H_2S and KCN etching as measured by XRF (Appendix VII.iii). The thin films have been prepared from stacks of Spray ILGAR $Cu_{2-x}S$ and $In_2(O,S)_3$ layers as described in Fig. 3.9a-c. The absolute uncertainties of the elemental contents are ± 1 % the relative uncertainties of the thickness and deposition rates are ± 15 %. The detailed deposition parameters are listed in Appendix I.

Sample	**325**	**326**	**327**	**328**
Copper content [at. %]	25	24	24	23
Indium content [at. %]	26	25	24	27
Sulfur content [at. %]	50	51	51	50
Thickness [nm]	713	1053	322	465
Deposition rate [nm/min]	20	33	13	18

These values agree well with the composition of $CuInS_2$. The films are slightly indium-rich (1 %), which has also been observed in KCN etched $CuInS_2$ thin films used in highly efficient thin-film solar cells [Hashimoto '95; Camus_1 '08]. The thickness and the deposition rates of these films vary by more than a factor of three. The highest thickness and rate was achieved if $Cu_{2-x}S$ was deposited prior to $In_2(O,S)_3$ (sample 326, Fig. 3.9b), whereas the lowest values were obtained for the films, in which $Cu(hfac)_2$ and $InCl_3$ were sprayed within one ILGAR-cycle (samples 327 and 328, Fig. 3.9c). Besides for sample 327, the deposition rates are in the range that was desired for the deposition of $CuInS_2$ thin films within their relative error of ± 15 % (20-30 nm per minute). However, at this point it is not clear, if the films indeed consist of $CuInS_2$ or if phases like In_2O_3, In_2S_3 or $Cu_{2-x}S$ are also present. Therefore, samples 325-328 were investigated by grazing incidence XRD (0.5 °). In Fig. 3.10a, the diffractograms of these films are shown.
Besides molybdenum (from the substrate; JCPDS 00-042-1190), $CuInS_2$ is the only detected phase, of which the chalcopyrite-type (JCPDS 00-027-0159) and CuAu-ordered (Fig. 2.5; [Alvarez-Garcia '02]) modifications are identified. For CuAu-ordered $CuInS_2$, only the {001} reflection is indicated, since all other reflections of this phase coincide with reflections of the chalcopyrite phase [Alvarez-Garcia '02]. This shows that $Cu_{2-x}S$ and In_2S_3 indeed formed $CuInS_2$ in all samples, as it was expected from the phase diagram (Fig. 2.4). In particular, no In_2O_3 (JCPDS 00-006-0416) was detected. This means that the Ar/H_2S annealing led to a complete sulfurization of all In_2O_3, which was present in the $In_2(O,S)_3$ thin films (section 3.2.). In the diffractogram in Fig. 3.10a, the contribution of the molybdenum {110}-reflection strongly differs for the samples 325-328. The diffractograms were obtained in gracing incidence mode at an angle of 0.5 °. Assuming an X-ray absorption coefficient of 730 cm^{-1} for

$CuInS_2$ only the first 500 nm of the samples are probed in this mode [Neisser_2 '01]. Consequently, the thickness of samples 327 and 328 must be below 500 nm, whereas samples 325 and 326 are thicker. This agrees well with the XRF-measurements (Table 3.7) and supports the validity of these data.

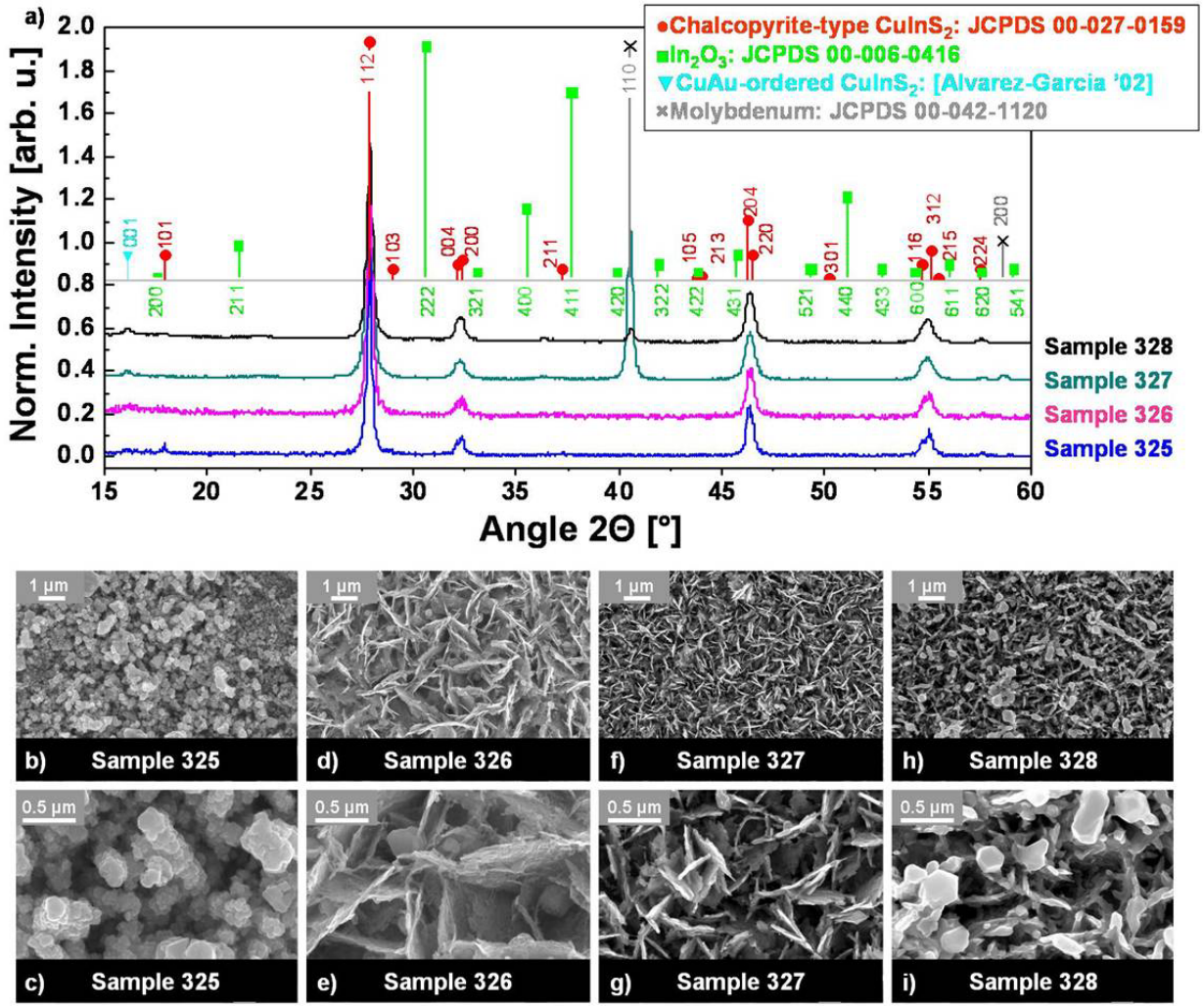

Fig. 3.10: a) Diffractograms of sequentially deposited ILGAR $CuInS_2$ thin films (samples 325-328; Fig. 3.9). After deposition, the films were annealed in Ar/H_2S and etched in KCN (Appendix I). The diffractograms are normalized with respect to the {112}-reflection of chalcopyrite-type $CuInS_2$ and shifted on the intensity axis for the sake of clarity. The colored lines indicate the contributions of various crystalline phases: red circles: Chalcopyrite-type $CuInS_2$ (JCPDS: 00-027-0159), green squares: In_2O_3 (JCPDS: 00-006-0416), gray crosses: molybdenum (JCPDS: 00-042-1120) and cyan triangles: {001}-reflection of CuAu-ordered $CuInS_2$ [Alvarez-Garcia '02]. All other reflections of CuAu-ordered $CuInS_2$ overlap with chalcopyrite-type $CuInS_2$ reflections [Álvarez Garcia_1 '02]. b-i) Plan-view SEM images of samples 325 (b, c), 326 (d, e), 327 (f, g) and 328 (h, i).

The Spray ILGAR $CuInS_2$ thin films are meant to be used as absorber layers in planar thin-film solar cells. Such solar cell absorber layers (section 6.1.) need to have a compact morphology and a grain size in the range of 1-2 µm for optimum performance. Therefore, the morphology of samples 325-328 was investigated by SEM. In Fig. 3.10b-c (sample 325), d-e (sample 326), f-g (sample 327) and h-i (sample 328) planar SEM images of these thin films are shown. The images were obtained after the post-deposition Ar/H_2S annealing and KCN etching. All samples exhibit a porous and highly structured morphology. In the case of samples 326-328 this morphology is similar to the highly structured morphology of the Spray ILGAR $In_2(O,S)_3$ thin film (sample 324, Fig. 3.8). However, the XRF (Table 3.7) and XRD (Fig. 3.10a) results showed that the films consist of $CuInS_2$. Hence, these results indicate that

$CuInS_2$ is formed from In_2S_3 and $Cu_{2-x}S$ mainly by interdiffusion of the elements without a recrystallization of the entire film and thus no observable changes of the morphology can be observed.
Such highly facetted growth regimes are often observed for spray deposition at high temperatures [Schoonmann '00]. It has been shown, however, in section 3.1.1. that a high substrate temperature is needed in order to achieve a sufficient deposition rate (20-30 nm per minute) in the Spray ILGAR process. Thus, it has to be concluded that the sequential deposition of $CuInS_2$ thin films by the Spray ILGAR process, does not yield compact $CuInS_2$ thin films, as they are needed for application as solar cell absorber films in planar thin-film solar cells. However, it was shown that the films consist of $CuInS_2$ and can be deposited at deposition rates of up to 30 nm per minute. Hence, such films could possibly be applied in solar cell systems, in which highly structured material is needed, such as eta-solar cells [Kaiser '01].

3.3.2. Simultaneous Deposition of Spray ILGAR $CuInS_2$ Thin Films

In this section, a Spray ILGAR process for the preparation of $CuInS_2$ thin films from a mixed acetone solution of $Cu(hfac)_2$ and $InCl_3$ is investigated. In contrast to the sequential process described in the previous section, in this process both cation species (indium and copper) are provided simultaneously. After deposition, these films were annealed in an Ar/H_2S gas mixture and etched in KCN. The samples were characterized by XRF, XRD and SEM. By this process, it was possible to deposit compact $CuInS_2$ thin films.

Since the influence of the [Cu]:[In] ratio of the spraying solutions on the [Cu]:[In] ratio of the deposited thin film was unknown, two samples have been prepared from mixed solutions of $Cu(hfac)_2$ and $InCl_3$/acetone solutions with different [Cu]:[In] ratios. One sample (sample 329) was prepared from a solution of a [Cu]:[In] ratio of one. Therefore, 25 ml of a 40 mM $Cu(hfac)_2$/acetone solution and 25 ml of a 40 mM $InCl_3$/acetone solution were mixed and sprayed until they were consumed completely. A second sample (sample 330) was prepared using a copper-rich solution (25 ml of a 40 mM $Cu(hfac)_2$/acetone solution and 20 ml of a 40 mM $InCl_3$/acetone solution, [Cu]:[In] = 1.25). All other deposition parameters were identical to those in Table 3.6 and the setup shown in Fig. 3.3 was used for both samples.
The composition of samples 329 and 330 was investigated by XRF directly after deposition, i.e. without any post-deposition annealing or KCN etching. For both samples similar relative copper, indium and sulfur contents (sample 329: 31 ± 1 at. % copper, 29 ± 1 at. % indium, 40 ± 1 at. % sulfur; sample 330: 31 ± 1 at. % copper, 28 ± 1 at. % indium, 41 ± 1 at. % sulfur) were determined. These compositions deviate strongly from the stoichiometry of $CuInS_2$. This indicates the presence of secondary phases like $Cu_{2-x}S$ and In_2O_3 as they were found in the sequentially deposited Spray ILGAR $CuInS_2$ thin films (section 3.3.1.). Therefore, both films were cut in two halves, of which one was left untreated (“as-deposited”) and one was annealed for 45 min at 375 °C in Ar and 15 min at 550 °C in a 95 % Ar / 5 % H_2S gas mixture [Kropp '02] and etched in KCN (“H_2S/KCN”) [Scheer '94; Scheer '95]. In Table 3.8 the relative copper, indium and sulfur contents are listed (in atomic percent). It can be seen that after the H_2S and KCN treatments the composition agrees within 1 % to that of KCN etched RTP-$CuInS_2$ thin films (24 ± 1 % copper, 26 ± 1 % indium, 50 ± 1 % sulfur; [Hashimoto '95; Camus_1 '08]). The thickness of the films was determined as 1034 ± 155 nm (sample 329) and 743 ± 111 nm (sample 330), which corresponds to deposition rates of 37 ± 5 nm per minute and 29 ± 4 nm per minute. Hence, for both samples the deposition rate is in or even above the aimed range for the deposition of $CuInS_2$ thin films. The reduced thickness of sample 330 is due to the fact that less (20 ml instead of 25 ml) $InCl_3$/acetone solution was used in the deposition process.

Table 3.8: Relative copper, indium and sulfur content (in atomic percent) and thickness (assuming a $CuInS_2$ bulk density of 4.75 g/cm^3 [www_4 '08]) of Spray ILGAR $CuInS_2$ thin films (samples 329 and 330) (as-deposited and after annealing in Ar/H_2S and KCN etching [Scheer '94; Scheer '95; Kropp '02]) as measured by XRF (Appendix VII.iii). The thin films were prepared by spraying of a mixed solution of $Cu(hfac)_2$ and $InCl_3$/acetone solutions using the setup shown in Fig. 3.3. The deposition parameters listed in Table 3.6 have been used. The uncertainties of the elemental contents are ± 1 % (absolute). The uncertainties of the thickness and the deposition rates are ± 15 % (relative).

	Sample 329		Sample 330	
	As-deposited	H_2S / KCN	As-deposited	H_2S / KCN
Copper content [at. %]	31	24	31	24
Indium content [at. %]	29	27	28	26
Sulfur content [at. %]	40	49	41	50
Thickness [nm]	-	1034	-	743
Deposition rate [nm/min]	37		29	

The structural properties of samples 329 and 330 were investigated by grazing incidence XRD (0.5 °). In Fig. 3.11, the diffractograms of both films are shown as obtained directly after deposition (Fig. 3.11a) and after the H_2S and KCN post-deposition treatments (Fig. 3.11b).

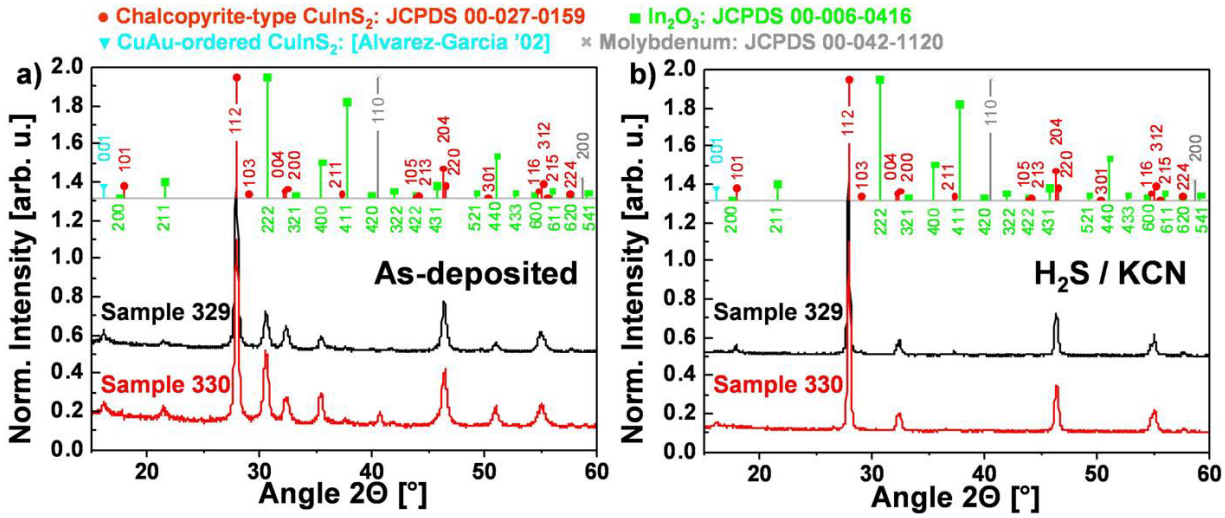

Fig. 3.11: X-ray diffractograms of as-deposited and H_2S and KCN treated Spray ILGAR $CuInS_2$ thin films prepared from mixed $Cu(hfac)_2$ and $InCl_3$ acetone solutions of [Cu]:[In] ratios of 1.0 (sample 329; black upper trace) and 1.25 (sample 330; red lower trace) in the as-deposited state (a) and after Ar/H_2S annealing and KCN etching (b). The diffractograms are normalized with respect to the {112}-reflection of chalcopyrite-type $CuInS_2$ and shifted on the intensity axis for the sake of clarity. The colored lines indicate the reflections of different crystalline phases: red: Chalcopyrite-type $CuInS_2$ (JCPDS: 00-027-0159), green: In_2O_3 (JCPDS: 00-006-0416), gray: molybdenum (JCPDS: 00-042-1120) and cyan: {001}-reflection of CuAu-ordered $CuInS_2$ [Alvarez-Garcia '02]. All other CuAu-ordered $CuInS_2$ reflections overlap with chalcopyrite-type $CuInS_2$ reflections [Álvarez Garcia_1 '02]. See Appendix I for preparation parameters.

As for sequentially deposited Spray ILGAR $CuInS_2$ thin films, after deposition the films consist of $CuInS_2$ (chalcopyrite-type and CuAu-ordered) and In_2O_3. In sample 330, the In_2O_3 contributions are stronger than in sample 329, even though less $InCl_3$/acetone solution was used for the preparation of sample 330. No crystalline $Cu_{2-x}S$ phases were detected in the samples by XRD. In the as-deposited sample 330, a small contribution of the molybdenum {110}-reflection is found, which is due to the smaller thickness of the film. After H_2S and KCN treatments (Fig. 3.11b), only $CuInS_2$ (chalcopyrite-type and CuAu-ordered) was identified in both films. In contrast to sample 329, the {101}- and {103}-reflections of chalcopyrite-type $CuInS_2$ could not be detected in sample 330 after the H_2S and KCN treatments. This indicates a higher degree of crystalline order in sample 329, which was deposited from a spraying solution of a [Cu]:[In] ratio of one (sample 330: [Cu]:[In]=1.25)

and contrasts results obtained from PVD- and RTP-prepared $CuInS_2$ thin films, for which an increased crystalline order was observed for copper-rich preparation [Scheer '93; Klenk '97]. In order to further assess the structural properties of the Spray ILGAR $CuInS_2$ thin films (samples 329, 330), their morphology was studied by SEM (Fig. 3.12).

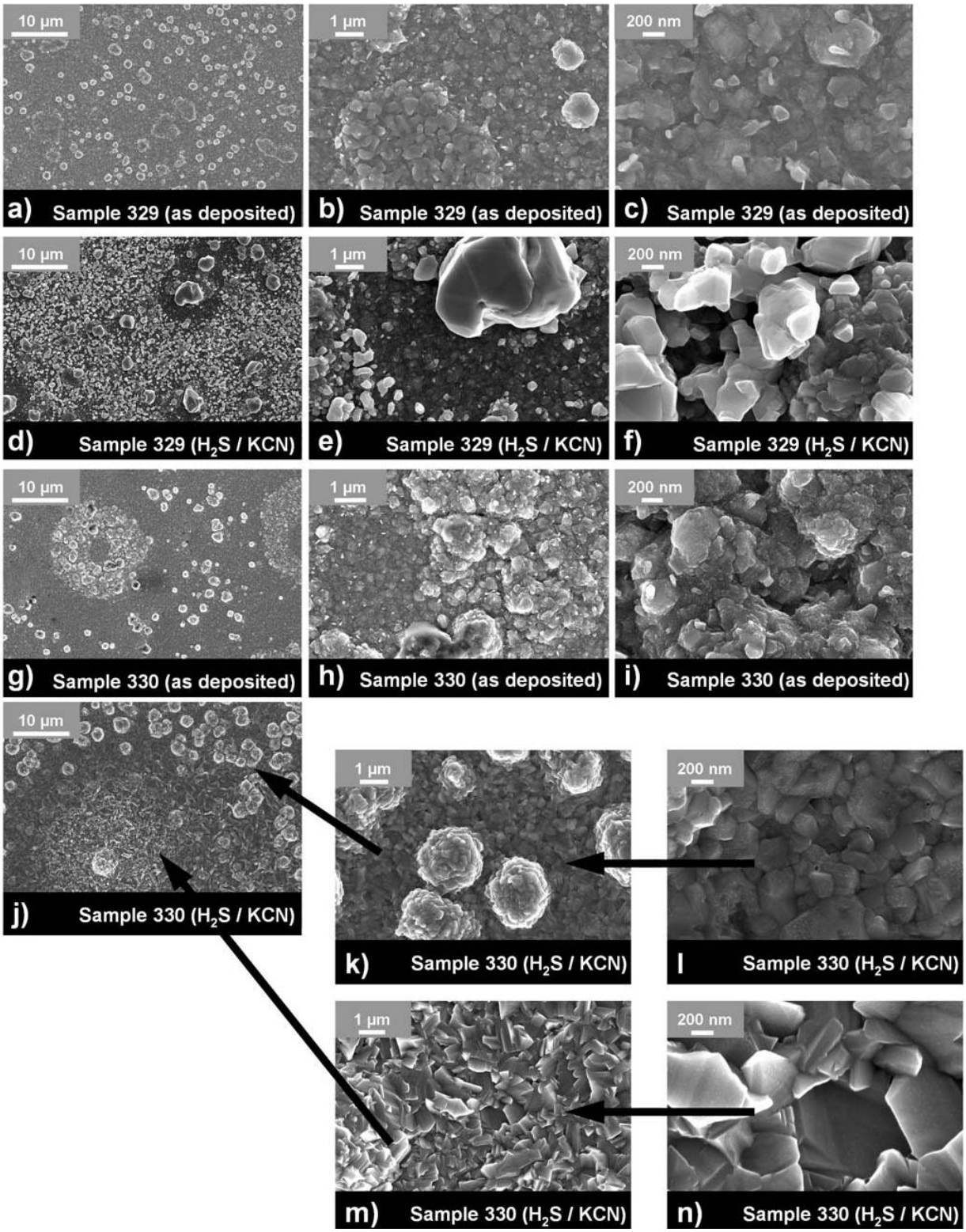

Fig. 3.12: Plan-view SEM images of as-deposited and H_2S and KCN treated Spray ILGAR $CuInS_2$ thin films prepared from mixed $Cu(hfac)_2/InCl_3$ acetone solutions of [Cu]:[In] ratios of 1.0 (sample 329) and 1.25 (sample 330): Sample 329: a-c) as-deposited and d-f) H_2S and KCN treated. Sample 330: g-i) as-deposited and j-n) H_2S and KCN treated sample 330. See Appendix I for preparation parameters.

In Fig. 3.12, plan-view SEM-images of both films are shown as they were obtained after deposition (sample 329: Fig. 3.12a-c; sample 330: Fig. 3.12g-i) and after the H_2S and KCN post-deposition treatments (sample 329: Fig. 3.12d-f; sample 330: Fig. 3.12j-n). All samples show a compact morphology without voids, which is a prerequisite for their application as solar cell absorber films in planar thin-film solar cells (section 6.1.). Additionally, both films have an inhomogeneous surface with scattered islands. For sample 329 ([Cu]:[In] = 1), these islands seem to be statistically distributed over the surface, whereas they are agglomerated forming circular patterns on the surface of sample 330 ([Cu]:[In] = 1.25). In the as-deposited films (sample 329: Fig. 3.12a-c; sample 330: Fig. 3.12g-i), these islands are similar to CuS islands observed by Walter *et al.* on coevaporated $CuInS_2$ thin films [Walter '96]. Thus, these islands may also consist of CuS or another copper sulfide phase. The rest of the surface consists of homogeneous grains with a size of up to 200 nm for both films.
Upon H_2S and KCN treatments, large (diameters of several µm) crystallites are found on the surface of sample 329 (Fig. 3.12d-f), whose distribution is similar to that of the islands on the as-deposited sample 329 (Fig. 3.12a-c). The rest of the film surface consists of grains of diameters of 100-300 nm. For sample 330, two regions of different morphologies can be distinguished: Some regions (Fig. 3.12k-l) of the film consist of grains with smooth edges (diameters of about 200-700 nm). These grains form three-dimensional clusters (diameters of about 2-3 µm; Fig. 3.12k), which are distributed statistically over the surface. In other regions (Fig. 3.12m-n), sharp-edged grains with diameters of up to 1 µm are found. In view of the application of the Spray ILGAR $CuInS_2$ thin films as solar cell absorbers in planar thin-film solar cells, the morphology observed for sample 330 ([Cu]:[In] = 1.25) after H_2S and KCN post-deposition treatments may be more favorable than that of sample 329 ([Cu]:[In] = 1) due to the larger average grain size and the more homogeneous grain size distribution of sample 330. According to the XRD results shown above, sample 329 appeared to exhibit a higher degree of crystalline order than sample 330. The SEM results, however, indicate that this was likely due to the presence of the large crystallites that are scarcely distributed over the sample surface. In grazing incidence XRD measurements the contributions of these crystallites can be assumed to dominate the diffractogram, even though the rest of the volume of sample 329 consists of grains smaller than those of sample 330.
So far, only the surface morphology of samples 329 ([Cu]:[In] = 1) and 330 ([Cu]:[In] = 1.25) was investigated (Fig. 3.12). In order to study how their morphology evolves in depth, also the cross-sections of these samples have been characterized by SEM. In Fig. 3.13, SEM images of the cross-sections of the as-deposited and H_2S and KCN treated samples 329 (Fig. 3.13a: as-deposited, Fig. 3.13b: H_2S and KCN treated) and 330 (Fig. 3.13c: as-deposited, Fig. 3.13d: H_2S and KCN treated) are shown. Both as-deposited samples look similar and consist of numerous layers of an approximate thickness of about 20-30 nm. Some of these layers are indicated by the dotted lines in Fig. 3.13a. It was found that the number of these layers corresponds to the number of ILGAR-cycles that were used for the deposition process of the respective thin films (24 ILGAR-cycles for sample 329; 22 ILGAR-cycles for sample 330). Thus, it may be assumed that for some reason, layers, which were deposited in separate ILGAR-cycles, do not grow together during the ILGAR-process. To reveal the origin of this behavior is one of the main topics of this thesis. The post-deposition H_2S annealing and KCN etching modified this layered morphology of the films only slightly, such that some of the layers grew together. Additionally, another several hundred nanometers thick layer formed during these treatments upon the *layered bottom layer* (Fig. 3.13b and d). This upper *well-crystallized top layer* consists of grains with diameters in the range of several hundred nanometers. Note that the images in Fig. 3.13a-d are all shown using the same magnification. This means that the thickness of the *layered bottom layer* of the film did not change during these treatments and the *well-crystallized top layer* was formed additionally. Hence, it may be assumed that material diffused out of the thin films during the post-deposition treatments and

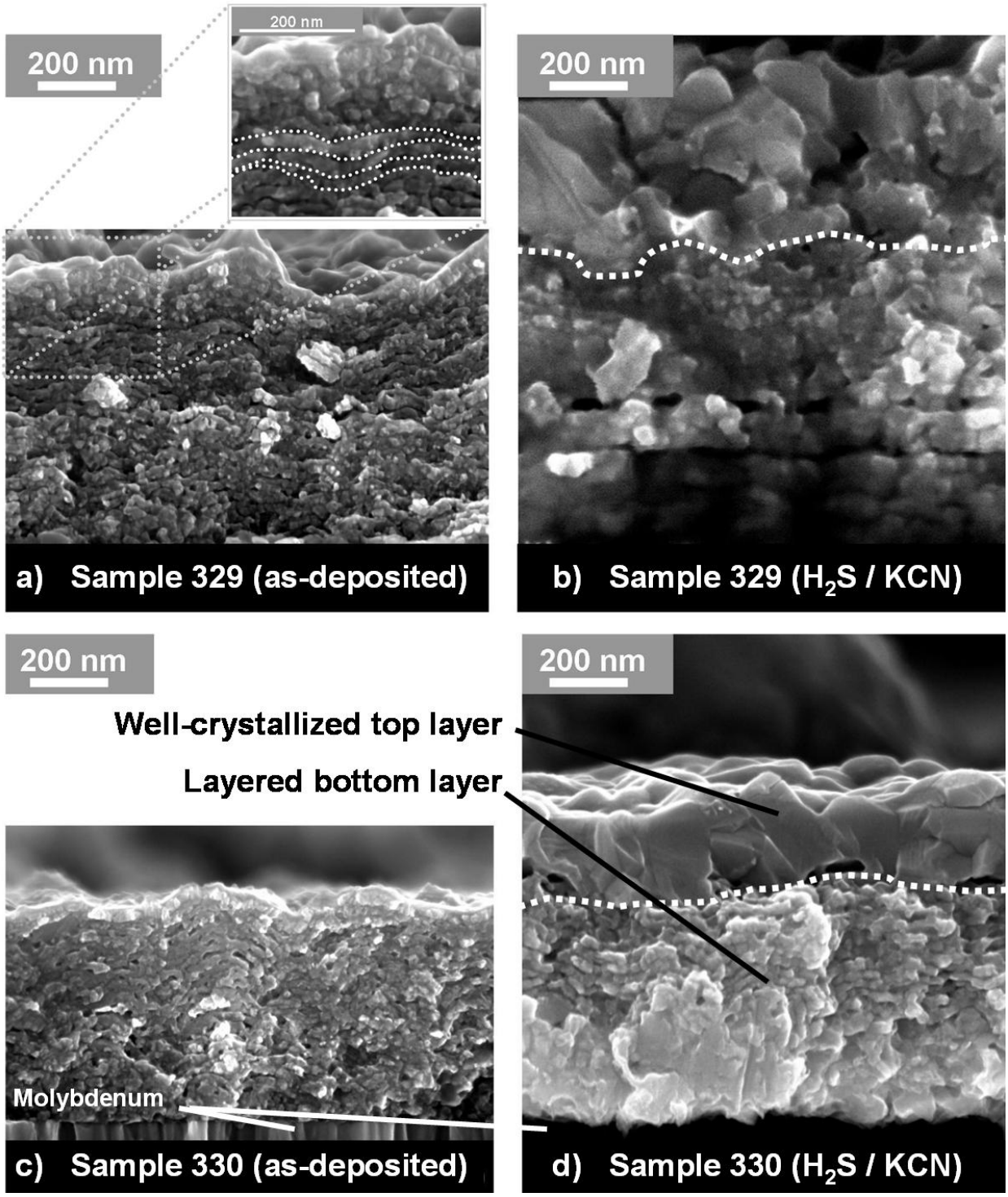

Fig. 3.13: SEM images of the cross-section of two as-deposited (a and c) and H_2S and KCN treated (b and d) Spray ILGAR $CuInS_2$ thin films that were prepared from mixed $Cu(hfac)_2$ and $InCl_3$ / acetone solutions of different [Cu]:[In] ratios (a-b: sample 329: [Cu]:[In] =1; c-d: sample 330: [Cu]:[In] =1.25). The dotted lines serve as a guide to the eye and separate different regions of the thin films. The films were deposited using the setup shown in Fig. 3.3. See Appendix I for preparation parameters.

thus led to the formation of the additional *well-crystallized top layer* on top of the *layered bottom layer*. However, at this point the mechanisms, which lead to the formation of the *well-crystallized top layer* and hinder the formation of a compact layer in the *layered bottom layer*, remain unclear and will be the focus of chapter 4.

In view of the desired application of the Spray ILGAR $CuInS_2$ thin films as absorber layers in thin-film solar cells, the formation of the *well-crystallized top layer* in the H_2S and KCN

treated films may be advantageous, since most charge carriers in such a device are generated in the direct vicinity of the buffer-absorber-interface (section 6.1.). Therefore, the crystalline properties in this region are most important for a solar cell. This is exactly the region, in which the simultaneously deposited Spray ILGAR $CuInS_2$ thin films exhibit the largest grain size and thus the best crystal quality. However, it would still be desirable if also the *bottom layer* of the H_2S and KCN treated films showed the same well-crystallized morphology that is observed in the *top layer*. It was found in further studies that this peculiar layered morphology did not depend on the choice of specific preparation parameters (see samples investigated in chapter 4). Neither a variation of the durations of the spray- and H_2S steps in the ILGAR-cycles nor a variation of the [Cu]:[In] ratio of the spraying solution or of the post-deposition annealing yielded thin films with a morphology, which was principally different from that of samples 329 and 330. Since an understanding of the mechanisms, which determine the morphology of the Spray ILGAR thin films, is regarded as a prerequisite for the improvement of the film morphology, the growth process of the Spray ILGAR thin films is analyzed in detail in chapter 4.

3.4. Summary of Chapter 3

In this chapter, the development of a process for the deposition of $CuInS_2$ thin films based on the Spray ILGAR method was described. Therefore, a new Spray ILGAR process for the deposition of copper sulfide thin films was developed, by modifying and extending the setup used by Allsop *et al.* for the deposition of In_2S_3 thin films [Allsop_1 '06], which did not allow for the deposition of any copper-containing compounds. This was done by choosing an appropriate copper-containing precursor compound ($Cu(hfac)_2$) and solvent (acetone). Additionally, a preheating of the aerosol was implemented. Thus, the deposition of copper sulfide thin films at a rate of up to 11 ± 2 nm per minute could be realized (section 3.1.). Subsequently, it was shown that the same Spray ILGAR process could be used for the deposition of $In_2(O,S)_3$ thin films (section 3.2.). In section 3.3., both processes were combined in order to deposit Spray ILGAR $CuInS_2$ thin films. Here, two different approaches were examined. In a first approach, bilayer stacks of various stacking sequences of Spray ILGAR copper sulfide and $In_2(O,S)_3$ were deposited sequentially and annealed in an Ar/H_2S atmosphere subsequently (section 3.3.1.). Thus, highly structured $CuInS_2$ thin films could be prepared at a rate of up to 20-30 nm per minute. However, since the Spray ILGAR $CuInS_2$ thin films were meant to be used as absorber films in planar solar cells a compact morphology was desired. Such a morphology could be realized by using mixed spraying solutions of $Cu(hfac)_2$ and $InCl_3$ in acetone (section 3.3.2.). These films had a compact multi-layered structure and could be deposited at a rate of up to 20-30 nm per minute. Upon annealing of such films in an Ar/H_2S atmosphere a bilayer structure was achieved, which consisted of a nanocrystalline *layered bottom layer* and a *well-crystallized top layer* (grain sizes of several hundred nanometers). Generally, this morphology was regarded to be promising for the desired applications of the films as absorber layers in planar thin-film solar cells. At this point the origin of this morphology remains unknown. Hence, in the following chapter (chapter 4) the mechanisms that govern the growth of the Spray ILGAR $CuInS_2$ will be investigated, in order to deduce a growth model.